Quasitransverse momentum dependent distributions at next-to-next-to-leading order

Óscar del Río and Alexey Vladimirov

Departamento de Física Teórica and IPARCOS, Universidad Complutense de Madrid, E-28040 Madrid, Spain

(Received 29 May 2023; accepted 17 November 2023; published 13 December 2023)

The partons' transverse momentum can be explored with QCD lattice simulations by studying the quasitransverse-momentum-dependent parton distribution functions (qTMDPDFs), which are factorized in terms of physical TMDPDFs and soft factors in the limit of the large hadron's momentum. We present the next-to-next-to-leading order (NNLO) calculation of the coefficient function for this factorization. Together with already known expressions for anomalous dimensions, this result allows analysis of lattice data at NNLO perturbative accuracy.

DOI: 10.1103/PhysRevD.108.114009

I. INTRODUCTION

Extraction of parton distribution and related quantities from the lattice simulations is a rapidly growing direction of QCD. The central tool for such extractions is the factorization theorems derived in the large hadron's momentum regime. Combining various equal-time operators and hadron states, one is accessing a variety of parton distributions [1,2]. In this work, we study the so-called quasitransverse momentum dependent (qTMD) parton distribution functions (PDFs) [2,3]. The corresponding matrix element is defined as (we use the notation of Ref. [4])

$$\tilde{\Omega}^{ij}_{\text{bare}}(y) = \langle P|\bar{q}^j(y)[y;b+Lv][b+Lv;Lv][Lv;0]q^i(0)|P\rangle, \quad (1)$$

where $|P\rangle$ is the (possibly polarized) hadron state with momentum P, q is the quark field, v and y are spacelike vectors (with $y^0 = v^0 = 0$), and $b^\mu = y^\mu - v^\mu(vy)/v^2$. The expression $[a,b]$ represents a straight gauge link from point a to point b. The operator represents a quark-antiquark pair separated by y and connected by a staple-shaped Wilson line along direction v^μ and of size L.

In the regime of the large momentum hadron P and the large length of gauge-link staple L, the qTMD matrix element (1) can be expressed via the physical TMD distribution through the factorization theorem [see Eq. (4)], derived using various approaches in Refs. [4–10]. A feature of the qTMD factorization theorem is that in addition to the physical transverse-momentum-dependent parton distribution functions (TMDPDF), it contains an extra function Ψ that accumulates the nonperturbative interaction between the parts of the staple gauge link (also called intrinsic soft factor [6]). The treatment of this function is slightly different in different approaches (compare, e.g., Refs. [7–9]), but conceptually the factorization theorem is the same in all cases. The main perturbative ingredient is the coefficient function, which is currently known at next-to-leading order (NLO) [8,11].

The operator (1) is localized in the equal-time plane, and thus the qTMD matrix element can be simulated within lattice QCD. The results of the simulations can be combined such that the functions Ψ cancel. In this way, one determines the nonperturbative Collins-Soper kernel (see Refs. [11–16]). Alternatively, the Ψ function can be determined from the auxiliary procedure [6], and then one accesses the TMDPDF distribution [17]. The precision of extraction crucially depends on the accuracy of the perturbative input, which is currently limited by the knowledge of the hard coefficient function. Importantly, this coefficient function is universal and is the same for all polarized quasi-TMDPDF of the leading power [8,9], and it is independent of the particularities of the nonperturbative definition of the internal soft factor.

Nowadays, the extractions of TMDPDFs from the data are routinely performed at next-to-next-to-leading order (NNLO) or N^{3}LO order (see, for example, [18–20]), and recently were pushed to N^{4}LO order [21]. It has been demonstrated [18,20,22] that (at least) NNLO is required since the NLO is not sufficiently precise to describe the data from the modern experiments. Modern lattice simulations of quasi-transverse-momentum-dependent parton

distribution functions (qTMDPDFs) have yet to reach that order of precision. Still, nonetheless, the NNLO contribution is sizable since the typical scale of lattice simulations is about 1–3 GeV. In this paper, we present the expression for the hard coefficient function for the factorization of qTMDPDF at NNLO. Other perturbative ingredients of the factorization theorem (anomalous dimensions) are known at NNLO and higher. Therefore, using the result of this work, one could analyze the lattice data at complete NNLO.

II. FACTORIZATION THEOREM

The factorization theorem connecting qTMDPDFs and physical TMDPDFs is discussed in many articles [4–10], which we refer to for detailed discussion. Different spinor components of qTMDPDF correlator (1) obey different kinds of factorization theorems [23]. The projection to desired components is done by a contraction with appropriate Dirac matrix

$$\tilde{\Omega}^{[\Gamma]}(y) = \frac{1}{2}\Gamma_{ji}\tilde{\Omega}^{ij}(y). \tag{2}$$

The most interesting cases are the components projected by $\Gamma \in \Gamma_+ = \{\gamma^+, \gamma^+\gamma^5, i\sigma^{\alpha+}\gamma^5\}$, where n^μ is a lightlike vector $n^2 = 0$ defined by the decomposition of hadron's momentum $P^\mu = \bar{n}^\mu P^+ + n^\mu M^2/2P^+$ $(P^2 = M^2)$. For definiteness, we fix

$$v^\mu = \frac{n^\mu - \bar{n}^\mu}{\sqrt{2}}, \tag{3}$$

with $v^2 = -1$. The components projected by $\Gamma \in \Gamma_+$ obey the leading-power factorization theorem

$$\Omega^{[\Gamma]}(x,b,\mu) = \mathbb{C}_{11}(\mathbf{L}_p, a_s(\mu))\Psi(b;\mu,\bar{\zeta})\Phi_{11}^{[\Gamma]}(x,b;\mu,\zeta) + \mathcal{O}\left(\frac{M^2}{x^2(vP)^2}, \frac{1}{b^2(vP)^2}, \frac{b}{L}, \frac{1}{ML}\right), \tag{4}$$

where

$$\Omega^{[\Gamma]}(x,b;\mu) = \int_{-\infty}^{\infty}\frac{dy_v}{2\pi}e^{-ixy_v(vP)}\tilde{\Omega}^{[\Gamma]}_{q/h}(y,b;\mu), \tag{5}$$

$$\Phi_{11;\text{bare}}[\Gamma](x,b;\mu,\zeta) = \int_{-\infty}^{\infty}\frac{d\lambda}{2\pi}e^{-ix\lambda P_+}\langle P|\bar{q}(\lambda n + b)[\lambda n + b; b + sn\infty]\frac{\Gamma}{2}[sn\infty; 0]q(0)|P\rangle, \tag{6}$$

$$\Psi_{\text{bare}}(b;\mu,\bar{\zeta}) = \langle 0|\frac{\text{Tr}}{N_c}[-\bar{n}\infty + b, b][b; b + Lv][b + Lv; Lv][Lv; 0][0, -\bar{n}\infty]|0\rangle \tag{7}$$

with $y^\mu = y_v v^\mu + b^\mu$,

$$\mathbf{L}_p = \ln(\mu^2/(2x(vP))^2), \tag{8}$$

and $a_s = g^2/(4\pi)^2$. The function $\Phi_{11}^{[\Gamma]}$ is the physical TMDPDF of twist-two. The direction of the Wilson lines s is defined by the direction of the staple contour $s = \text{sign}(L)$. In this way, different orientations of the staple contour give access to Drell-Yan or semi-inclusive deep-inelastic scattering (SIDIS) definitions of TMDPDFs, which can be used to test their universality [24,25]. We stress that the factorization limit is rather complicated [see the last term of (4)]. Explicitly, it requires $(vP), L \to \infty$ at fixed-finite x and b. We also note that at this power accuracy, there is no difference between v^-P^+ and $(vP) = P_z$, which is used as the hard scale.

The expression (4) is written in terms of renormalized functions. They are related to the bare functions as

$$\begin{aligned}
\Omega^{[\Gamma]}(x,b,\mu) &= Z_W^{-1}(\mu)Z_J^{-2}(\mu)\Omega^{[\Gamma]}_{\text{bare}}(x,b),\\
\Phi_{11}^{[\Gamma]}(x,b;\mu,\zeta) &= |Z_{U1}(\mu,\zeta)|^{-2}R^{-1}(b)\Phi^{[\Gamma]}_{11,\text{bare}}(x,b),\\
\Psi(b;\mu,\zeta) &= Z_{\Psi 1}(\mu,\zeta)^{-2}Z_W^{-1}(\mu)R^{-1}(b)\Psi_{\text{bare}}(b).
\end{aligned} \tag{9}$$

Here, the factor R renormalizes rapidity divergences (in most parts of schemes it is equal to the $S^{-1/2}$ where S is the TMD soft factor). The factor Z_J is the renormalization of the quark field in the axial gauge. The factors Z_{U1} and $Z_{\Psi 1}$ are ultraviolet (UV) renormalizations of the (leading-twist) semicompact operators constituting the TMD distributions [23]. Finally, the factor Z_W depends on b and L and accumulates all divergent factors associated with the staple contour, such as power divergences of spacelike links [26], cusps divergences at point $b + Lv$ and Lv, and other contributions [27]. Importantly, the same divergences happen in the function Ψ, and thus we do deal with them in our computation of the coefficient function.

The structure of divergences cancellation in the qTMD factorization theorem is similar to those in factorization of Drell-Yan or SIDIS. So, the rapidity divergences cancel in-between soft factor contributions, Φ_{11} and Ψ. The rapidity divergences leave no trace on the coefficient function, but introduce the rapidity scales ζ and $\bar{\zeta}$ (see details on Refs. [28–30]). The UV renormalization of TMD distributions cancels the infrared (IR) poles of the coefficient function. The cancellation happens only if

$$\zeta\bar{\zeta} = (2x\mu(vP))^2. \tag{10}$$

The UV poles are renormalized by Z_J's and result in the overall scaling of the qTMDPDF operator.

The scaling of functions (9) follows from their renormalization properties. For the Ω we have

$$\frac{d\ln\Omega^{[\Gamma]}(x,b,\mu)}{d\ln\mu^2} = 2\gamma_J + \gamma_W(b,L), \tag{11}$$

where γ_J is the anomalous dimension of the heavy-light current, and γ_W is the anomalous dimension associated with the renormalization of the staple link. The evolution of TMD distribution is [22,31]

$$\frac{d\ln\Phi_{11}^{[\Gamma]}(x,b;\mu,\zeta)}{d\ln\mu^2} = \frac{\Gamma_{\rm cusp}\ln(\frac{\mu^2}{\zeta}) - \gamma_V}{2}, \tag{12}$$

$$\frac{d\ln\Phi_{11}^{[\Gamma]}(x,b;\mu,\zeta)}{d\ln\zeta} = -\mathcal{D}(b,\mu), \tag{13}$$

where $\Gamma_{\rm cusp}$ is the anomalous dimension of the cusp of lightlike Wilson lines and $\mathcal{D}$ is the Collins-Soper kernel. The Collins-Soper kernel is a nonperturbative function, which represents the interaction of light quarks in the QCD vacuum environment [30]. Finally, the Ψ function also evolves with the pair of equations

$$\begin{aligned}\frac{d\ln\Psi(b;\mu,\zeta)}{d\ln\mu^2} &= \frac{\Gamma_{\rm cusp}}{2}\ln\left(\frac{\mu^2}{\zeta}\right) + 2\gamma_\Psi + \gamma_W(b,L),\\ \frac{d\ln\Psi(b;\mu,\zeta)}{d\ln\zeta} &= -\mathcal{D}(b,\mu),\end{aligned} \tag{14}$$

where γ_Ψ is the anomalous dimension associated with the finite part of the cusp anomalous dimension at the finite angle. The anomalous dimension[1] γ_Ψ was computed at LO in Ref.[2] [8], and the NLO term was computed in this work. We found that γ_Ψ coincides with the anomalous dimension associated with the heavy-quark [32] ($v^2 > 0$). This is not accidental, because the UV renormalization is insensitive to the sign of v^2, as it is proven in Ref. [33].

The expressions for anomalous dimensions $\Gamma_{\rm cusp}$, γ_J, γ_V, and γ_Ψ are well known. At N^{2}LO they can be found, e.g., in Refs. [33–35]. For the reader's convenience, we have collected all explicit expressions in Appendix A (A2)–(A5). The remaining anomalous dimension γ_W and the Collins-Soper kernel are not important in the present work.

III. QUASI-TMD DISTRIBUTION

The qTMD distribution is an artificial construction that reduces to the physical TMD distribution in the asymptotic limit $(vP) \to \infty$ and $L \to \infty$. Currently, there is no standard construction for this function (see discussion in Ref. [10]). Probably, the most popular way [4,5,7,9,11] is to consider the function

$$F^{[\Gamma]}(x,b;\mu) = \frac{\Omega^{[\Gamma]}(x,b,\mu)}{\Psi(b,\mu,\mu^2)}. \tag{15}$$

Using the factorization theorem (4), evolution equations. and condition (10), one finds

$$\begin{aligned}F^{[\Gamma]}(x,b;\mu) = &\left(\frac{(2x(vP))^2}{\zeta}\right)^{-\mathcal{D}(\mu)}\\ &\times \mathbb{C}_{11}(\mathbf{L}_p,\mu)\Phi_{11}^{[\Gamma]}(x,b;\mu,\zeta) + \cdots,\end{aligned} \tag{16}$$

where dots indicate the power corrections explicitly given in the last term of Eq. (4). Note that in this formulation the scaling equation for qTMD function is

$$\frac{d\ln F^{[\Gamma]}(x,b;\mu)}{d\ln\mu^2} = 2(\gamma_J - \gamma_\Psi) + \mathcal{D}(b,\mu). \tag{17}$$

The nonperturbative part of the subtraction factor could be different in other constructions, and it does not affect $\mathbb{C}_{11}$.

Generally speaking, the scales μ and ζ are independent; therefore, one can define a more general function

$$F^{[\Gamma]}(x,b;\mu,\zeta) = \frac{\Omega^{[\Gamma]}(x,b,\mu)}{\Psi(b,\mu,\zeta)}, \tag{18}$$

[1]By definition the anomalous dimension of the Ψ function is

$$\gamma_\Psi = -\frac{d\ln Z_\Psi}{d\ln\mu^2}.$$

Evaluating it one should take into account that $\zeta \sim \mu^2$, because μ is the only dimensional scale of the Ψ function. Therefore, $d\ln(\mu^2/\zeta)/d\ln\mu^2 = 0$. For the detailed discussion see Ref. [4].

[2]Reference [8] provides an incorrect expression for LO γ_Ψ. This mistake appeared due to the mismatch in definitions for the renormalization constant with earlier paper $Z_J \leftrightarrow Z_J^{-1}$. Once corrected, the expression for γ_Ψ coincides with the one computed here or in Ref. [4].

which reduces to (15) at $\zeta = \mu^2$. This function satisfies the pair of equations

$$\frac{d \ln F^{[\Gamma]}(x, b; \mu, \zeta)}{d \ln \mu^2} = 2(\gamma_J - \gamma_\Psi) - \frac{\Gamma_{\rm cusp}}{2} \ln\left(\frac{\mu^2}{\zeta}\right), \quad (19)$$

$$\frac{d \ln F^{[\Gamma]}(x, b; \mu, \zeta)}{d \ln \zeta} = +\mathcal{D}(b, \mu). \quad (20)$$

Note that the evolution with respect to ζ has an opposite sign in comparison to ordinary TMD evolution (12).

IV. COEFFICIENT FUNCTION

The qTMD operator can be written as a product $J_v^\dagger(y) \Gamma J_v(0)$, where the currents are

$$J_v^i(0) = [sv\infty, 0] q^i(0). \quad (21)$$

Structurally, the current J_v is similar to the renowned heavy-to-light current (see, e.g., [36]), with $v^2 = -1$, and an open spinor index. The separation between currents $y^2 \sim b^2$ is large in comparison to the hard scale $(vP)^{-1}$, and thus any exchange of perturbative gluons between currents is power suppressed [4,7–9]. This essentially simplifies the problem of computation of $\mathbb{C}_{11}$ and allows us to present it as

$$\mathbb{C}_{11} = |C_1|^2, \quad (22)$$

where C_1 is the coefficient function for the factorization of a current (21) into the leading-twist semicompact operators. Because of this structure, the coefficient function is independent of the Γ once $\Gamma \in \Gamma_+$. Therefore, it is universal for all eight leading-power components of the qTMDPDF matrix element.

Comparing the definitions (4), (9), and (22) we find that

$$C_1(\mathbf{L}_p, a_s(\mu)) = Z_J^{-1} C_{1,\rm bare} Z_{U1} Z_{\Psi 1}, \quad (23)$$

where we omit scaling arguments on the right-hand side for brevity. Note that the renormalization constant Z_{U1} and $C_{1,\rm bare}$ are complex valued in such an approach [23]. The renormalization constants Z_J, $Z_{\Psi 1}$, and Z_{U1} are known at N^{3}LO [33,35,37]. For our NNLO computation, we took the expressions from the appendixes and auxiliary files of Ref. [33] (for Z_J) and Refs. [34,38] (for Z_{U1}), and reconstructed from known anomalous dimension [35] (for $Z_{\Psi 1}$).

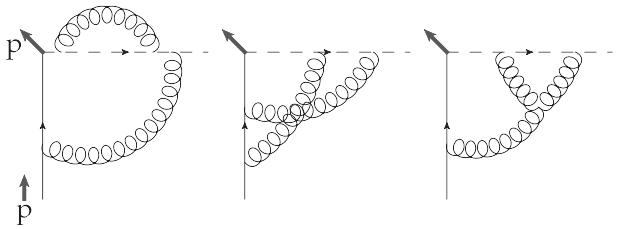

FIG. 1. Examples of diagrams contributing to C_1 at NNLO. The momentum p enters through the quark line and exits from the quark-Wilson line vertex, as indicated on the left diagram.

The examples of diagrams contributing to $C_{1,\rm bare}$ are shown in Fig. 1. Note that the same diagrams contribute to the computation of the matching coefficient of heavy-light quark current in the heavy-quark effective theory (HQEFT) [39]. The only difference between these computations is the sign of v^2 and that the momentum p is passing through the "light" quark line, while in the HQEFT matching coefficient computation, the momentum passes through the Wilson line. The computation is done in the dimensional regularization $d = 4 - 2\epsilon$. The reduction to the base integrals is performed by the FIRE6 library [40]. The result reads

$$C_{1\rm bare} = 1 + a_s X^\epsilon C_1^{(1)} + a_s^2 X^{2\epsilon} C_1^{(2)} + \mathcal{O}(a_s^3), \quad (24)$$

where $X = v^2/(2x(vP) - is0)^2$,

$$C_1^{(1)} = 2 C_F \Gamma(-\epsilon) \Gamma(2\epsilon) \frac{1-\epsilon}{1-2\epsilon}, \quad (25)$$

and the expression for $C_1^{(2)}$ is presented in Appendix A in Eq. (A1). Combining $C_{1\rm bare}$ with the renormalization factors (and renormalizing a_s), we observe the exact cancellation of $1/\epsilon$ poles. This provides a general check of the computation.

Substituting the renormalized expression for C_1 into Eq. (22), we obtain the NNLO coefficient function for the qTMD factorization theorem. It reads

$$\begin{aligned}
\mathbb{C}_{11} = 1 &+ a_s C_F(-\mathbf{L}_p^2 - 2\mathbf{L}_p - 4 + \zeta_2) + a_s^2 C_F \left\{ \frac{C_F}{2} \mathbf{L}_p^4 + \mathbf{L}_p^3 \left[2C_F - \frac{11}{9} C_A + \frac{2}{9} N_f \right] \right. \\
&+ \mathbf{L}_p^2 \left[C_F(6 - \zeta_2) + C_A\left(-\frac{100}{9} + 2\zeta_2 \right) + \frac{16}{9} N_f \right] + \mathbf{L}_p \left[C_F(4 + 26\zeta_2 - 24\zeta_3) \right. \\
&+ C_A\left(-\frac{950}{27} - \frac{22}{3}\zeta_2 + 22\zeta_3 \right) + N_f\left(\frac{304}{54} + \frac{4}{3}\zeta_2 \right) \Big] + C_F\left(-12 + 116\zeta_2 - 30\zeta_3 - \frac{475}{4}\zeta_4 \right) \\
&\left. + C_A\left(-\frac{3884}{81} - \frac{559}{18}\zeta_2 + \frac{241}{9}\zeta_3 + \frac{99}{2}\zeta_4 \right) + N_f\left(\frac{656}{81} + \frac{17}{9}\zeta_2 + \frac{2}{9}\zeta_3 \right) \right\} + \mathcal{O}(a_s^3), \quad (26)
\end{aligned}$$

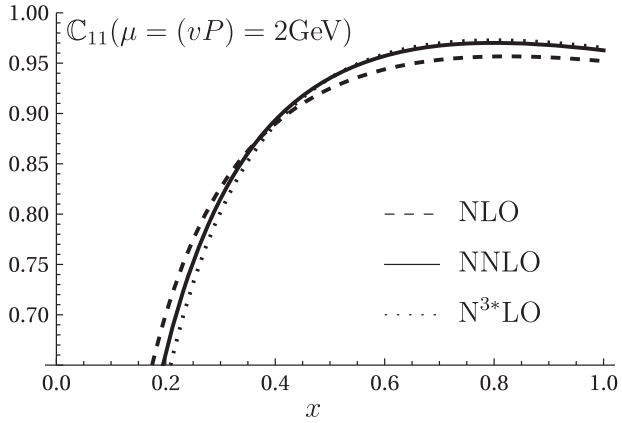

FIG. 2. Comparison of NLO, NNLO, and N^{3*}LO coefficient functions $\mathbb{C}_{11}$ as the function of x. The solid, dashed, and dotted lines represent the coefficient functions at NNLO, NLO, and N^{3*}LO, correspondingly. The comparison is done for the value of $(vP) = \mu = 2$ GeV, which is the typical setup for lattice computations.

where $\mathbf{L}_p$ is defined in Eq. (8), $C_F = (N_c^2 - 1)/2N_c$, $C_A = N_c$ are eigenvalues of the Casimir operator of $SU(N_c)$ algebra, N_f is the number of active quarks, and ζ_n is the Riemann ζ function. This expression is the main result of this paper. The NLO parts of the coefficient function and anomalous dimension γ_Ψ coincide with the known results [8,11].

The logarithm part of the coefficient function can be derived from the evolution equations defined above. It satisfies

$$\frac{d\ln \mathbb{C}_{11}}{d\ln \mu^2} = 2(\gamma_J - \gamma_\Psi) + \frac{\gamma_V}{2} - \frac{\Gamma_{\text{cusp}}}{2}\mathbf{L}_p. \tag{27}$$

Using explicit expressions for anomalous dimensions (A2)–(A5) we confirm this. Note that using this equation and (26) one is able to compute the logarithm part of the N^{3}LO coefficient function. We present it in Eq. (A6).

V. CONCLUSION

In this work, we have computed the coefficient function for the factorization of the qTMD matrix at NNLO. We have checked the cancellation of poles between renormalization factors and coefficient functions, which provides a check of the factorization theorem for the qTMD operator up to NNLO. These results also allow us to obtain the logarithm part of the N^{3}LO coefficient function. The intermediate and final expressions are also attached to the publication in the *Mathematica* format.

In Fig. 2 we present the comparison of NLO, NNLO, and N^{3*}LO coefficient functions at $(vP) = \mu = 2$ GeV (i.e., $\mathbf{L}_p = -2\ln x$), where 3* indicates that this coefficient function does not have the nonlogarithm term. At these energies, the coefficient function demonstrates a reasonable convergence for $x > 0.2$ (the NNLO term provides ∼5% correction at most). Below $x < 0.2$ the convergence drops rapidly; e.g., at $x = 0.1$ the NNLO correction is ∼20%, and N^{3*}LO is ∼40% (both in comparison to NLO). This shows the natural boundary $x \gtrsim 0.2$ for this approach. To access lower values of x one should find a way to improve the structure of the factorization theorem, either by resumming problematic logarithms (see discussion on a similar problem for the pseudo-PDF case [41]) or by matching with a different type of factorization theorem). The coefficient function is just multiplicative, and thus it is straightforward to update the existing procedures including the NNLO correction. It is also important that the coefficient function is independent of the polarization quantum numbers. Therefore, all eight leading-power TMD distributions can be considered at the same NNLO precision.

Note added.— In Ref. [42] the authors derived the same coefficient function at NNLO by studying the threshold logarithms and related functions. Their results agree with ours.

ACKNOWLEDGMENTS

We thank Ignazio Scimemi, Konstantin Chetyrkin, and Vladimir Braun for helpful discussions. We also thank Yizhuang Liu for spotting a misprint in the initial version of the manuscript and for helpful comments. A. V. is funded by the *Atracción de Talento Investigador* program of the Comunidad de Madrid (Spain) No. 2020-T1/TIC-20204. O. dR. is supported by the MIU (Ministerio de Universidades, Spain) fellowship FPU20/03110. This work is also supported by the Spanish Ministry Grant No. PID2019–106080GB-C21. A. V. also thanks the DFG FOR 2926 *Mercator Fellowship* for supporting the visit to Regensburg University, where a part of this work has been done.

APPENDIX A: EXPLICIT NNLO AND N^{3}LO EXPRESSIONS

1. Bare coefficient function

The bare coefficient function is defined in Eq. (24). Its NLO term is given in Eq. (25) in the closed form. The NNLO term for the bare coefficient function $C^{(2)}_{1\text{bare}}$ has a complicated form involving hypergeometric functions. Here, we present the expression expanded in ϵ. It reads

$$C_1^{(2)} = C_F e^{-2\epsilon\gamma_E}\left\{\frac{C_F}{2\epsilon^4}+\frac{1}{\epsilon^3}\left(C_F-\frac{11}{12}C_A+\frac{N_f}{6}\right)+\frac{1}{\epsilon^2}\left[C_F\frac{5}{2}(1+\zeta_2)+C_A\left(-\frac{133}{36}+\frac{\zeta_2}{2}\right)+\frac{11}{18}N_f\right]\right.$$
$$+\frac{1}{\epsilon}\left[C_F\left(5+12\zeta_2-\frac{25}{3}\zeta_3\right)+C_A\left(-\frac{673}{54}-\frac{143}{12}\zeta_2+\frac{11}{2}\zeta_3\right)+N_f\left(\frac{56}{27}+\frac{13}{6}\zeta_2\right)\right]$$
$$+C_F\left(4+\frac{145}{2}\zeta_2-\frac{59}{3}\zeta_3-\frac{321}{8}\zeta_4\right)+C_A\left(-\frac{3130}{81}-\frac{2089}{36}\zeta_2+\frac{395}{18}\zeta_3+\frac{159}{4}\zeta_4\right)$$
$$\left.+N_f\left(\frac{544}{81}+\frac{143}{18}\zeta_2-\frac{13}{9}\zeta_3\right)+\mathcal{O}(\epsilon)\right\}, \tag{A1}$$

where we extracted explicitly the $\overline{\text{MS}}$ factor.

2. Anomalous dimensions at NNLO

There are four anomalous dimensions appearing in this problem. Their NNLO expressions are

$$\Gamma_{\text{cusp}} = 4a_sC_F+4a_s^2C_F\left[C_A\left(\frac{67}{9}-2\zeta_2\right)-\frac{10}{9}N_f\right]$$
$$+4a_s^3C_F\left[C_A^2\left(\frac{245}{6}-\frac{268}{9}\zeta_2+\frac{22}{3}\zeta_3+22\zeta_4\right)+C_FN_f\left(-\frac{55}{6}+8\zeta_3\right)\right.$$
$$\left.+C_AN_f\left(-\frac{209}{27}+\frac{40}{9}\zeta_2-\frac{28}{3}\zeta_3\right)-\frac{4}{27}N_f^2\right]+\mathcal{O}(a_s^4), \tag{A2}$$

$$\gamma_V = -6a_sC_F+a_s^2C_F\left[C_F(-3+24\zeta_2-48\zeta_3)+C_A\left(-\frac{961}{27}-22\zeta_2+52\zeta_3\right)+N_f\left(\frac{130}{27}+4\zeta_2\right)\right]$$
$$+a_s^3C_F\left[C_F^2(-36\zeta_2-136\zeta_3-288\zeta_4+64\zeta_2\zeta_3+480\zeta_5-29)\right.$$
$$+C_FC_A\left(\frac{820}{3}\zeta_2-\frac{1688}{3}\zeta_3+\frac{988}{3}\zeta_4-32\zeta_2\zeta_3-240\zeta_5-\frac{151}{2}\right)+C_FN_f\left(-\frac{52}{3}\zeta_2+\frac{512}{9}\zeta_3-\frac{280}{3}\zeta_4+\frac{2953}{27}\right)$$
$$+C_A^2\left(-\frac{14326}{81}\zeta_2+\frac{7052}{9}\zeta_3-166\zeta_4-\frac{176}{3}\zeta_2\zeta_3-272\zeta_5-\frac{139345}{1458}\right)$$
$$\left.+C_AN_f\left(\frac{5188}{81}\zeta_2-\frac{1928}{27}\zeta_3+44\zeta_4-\frac{17318}{729}\right)+N_f^2\left(-\frac{40}{9}\zeta_2-\frac{16}{27}\zeta_3+\frac{4834}{729}\right)\right]+\mathcal{O}(a_s^4), \tag{A3}$$

$$\gamma_J = \frac{3}{2}a_sC_F+a_s^2C_F\left[C_F\left(-\frac{5}{4}+8\zeta_2\right)+C_A\left(\frac{49}{12}-2\zeta_2\right)-\frac{5}{6}N_f\right]$$
$$+a_s^3C_F\left[C_F^2\left(\frac{37}{4}-32\zeta_2+18\zeta_3+40\zeta_4\right)+C_FC_A\left(\frac{655}{72}+\frac{592}{9}\zeta_2-\frac{71}{3}\zeta_3+8\zeta_4\right)\right.$$
$$+C_FN_f\left(-\frac{235}{18}-\frac{112}{9}\zeta_2+\frac{44}{3}\zeta_3\right)+C_A^2\left(-\frac{1451}{216}-\frac{130}{9}\zeta_2+\frac{11}{3}\zeta_3+12\zeta_4\right)$$
$$\left.+C_AN_f\left(\frac{128}{27}+\frac{28}{9}\zeta_2-\frac{38}{3}\zeta_3\right)-\frac{35}{54}N_f^2\right]+\mathcal{O}(a_s^4), \tag{A4}$$

$$\gamma_\Psi = a_sC_F+a_s^2C_F\left[C_A\left(\frac{49}{9}-2\zeta_2+2\zeta_3\right)-\frac{10}{9}N_f\right]$$
$$+a_s^3C_F\left[C_A^2\left(\frac{343}{18}-\frac{304}{9}\zeta_2+\frac{370}{9}\zeta_3+22\zeta_4+4\zeta_2\zeta_3-18\zeta_5\right)+C_FN_f\left(-\frac{55}{6}+8\zeta_3\right)\right.$$
$$\left.+C_AN_f\left(-\frac{89}{27}+\frac{40}{9}\zeta_2-\frac{124}{9}\zeta_3\right)-\frac{4}{27}N_f^2\right]+\mathcal{O}(a_s^4). \tag{A5}$$

Here, the expressions for $\Gamma_{\rm cusp}$ and γ_V are taken from Ref. [43], the expression for γ_J is taken from Ref. [44], and the expression for γ_Ψ is taken from Ref. [35].

Using these expressions and Eq. (26), together with Eq. (27), we are able to determine the logarithmic part of the N^{3}LO coefficient function

$$\begin{aligned}
\mathbb{C}_{11}^{(3)} = C_F\Bigg\{&-\frac{C_F^2}{6}\mathbf{L}_p^6+\mathbf{L}_p^5\left[-C_F^2+\frac{11}{9}C_FC_A-\frac{2}{9}C_FN_f\right]\\
&+\mathbf{L}_p^4\left[C_F^2\left(-4+\frac{\zeta_2}{2}\right)+C_FC_A\left(\frac{122}{9}-2\zeta_2\right)-\frac{20}{9}C_FN_f-\frac{121}{54}C_A^2+\frac{22}{27}C_AN_f-\frac{2}{27}N_f^2\right]\\
&+\mathbf{L}_p^3\left[C_F^2\left(-\frac{16}{3}-26\zeta_2+24\zeta_3\right)+C_FC_A\left(\frac{1682}{27}+\frac{19}{9}\zeta_2-22\zeta_3\right)\right.\\
&\left.+C_FN_f\left(-\frac{254}{27}-\frac{10}{9}\zeta_2\right)+C_A^2\left(-\frac{2506}{81}+\frac{44}{9}\zeta_2\right)+C_AN_f\left(\frac{842}{81}-\frac{8}{9}\zeta_2\right)-\frac{64}{81}N_f^2\right]\\
&+\mathbf{L}_p^2\left[C_F^2\left(12-170\zeta_2+78\zeta_3+\frac{475}{4}\zeta_4\right)+C_FC_A\left(\frac{11996}{81}+\frac{2327}{18}\zeta_2-\frac{1429}{9}\zeta_3-\frac{89}{2}\zeta_4\right)\right.\\
&+C_FN_f\left(-\frac{2047}{162}-\frac{193}{9}\zeta_2+\frac{70}{9}\zeta_3\right)+C_A^2\left(-\frac{29351}{162}+\frac{26}{9}\zeta_2+\frac{220}{3}\zeta_3-22\zeta_4\right)\\
&\left.+C_AN_f\left(\frac{4469}{81}+\frac{16}{3}\zeta_2-\frac{16}{3}\zeta_3\right)+N_f^2\left(-\frac{292}{81}-\frac{8}{9}\zeta_2\right)\right]\\
&+\mathbf{L}_p\left[C_F^2\left(44-430\zeta_2+124\zeta_3+\frac{487}{2}\zeta_4+8\zeta_2\zeta_3+240\zeta_5\right)\right.\\
&+C_FC_A\left(\frac{5704}{81}+\frac{32521}{27}\zeta_2-\frac{6212}{9}\zeta_3-\frac{2450}{3}\zeta_4+6\zeta_2\zeta_3-120\zeta_5\right)\\
&+C_FN_f\left(\frac{6943}{162}-\frac{5374}{27}\zeta_2+\frac{244}{3}\zeta_3+\frac{350}{3}\zeta_4\right)+C_A^2\left(-\frac{723611}{1458}-\frac{21560}{81}\zeta_2+\frac{13858}{27}\zeta_3+260\zeta_4-\frac{112}{3}\zeta_2\zeta_3-100\zeta_5\right)\\
&\left.+C_AN_f\left(\frac{102683}{729}+\frac{6584}{81}\zeta_2-\frac{608}{9}\zeta_3-44\zeta_4\right)+N_f^2\left(-\frac{6184}{729}-\frac{128}{27}\zeta_2-\frac{16}{27}\zeta_3\right)\right]+c_3\Bigg\},
\end{aligned}\tag{A6}$$

where c_3 is the unknown finite part.

APPENDIX B: EVALUATION OF DIAGRAMS

In this appendix, we provide extra notes about the computation of diagrams for the coefficient function at NNLO. The examples of diagrams are shown in Fig. 1. In total, there are 10 diagrams (including self-energy graphs).

The momentum enters the diagram via the quark line and goes out in the vertex. There is no momentum incoming into the Wilson line. For example, the second diagram shown in Fig. 1 reads

$$\begin{aligned}
I = -g^4C_F\left(C_F-\frac{C_A}{2}\right)\int\frac{d^dk}{(2\pi)^d}\frac{d^dl}{(2\pi)^d}&\\
\times\frac{(\not P+\not k)\not v(\not P+\not l)\not v u(P)}{[(P+k)^2+i0][l^2+i0][(P+l)^2+i0]}&\\
\times\frac{1}{[(k-l)^2+i0][k\cdot v+i0][(k-l)\cdot v+i0]},&
\end{aligned}\tag{B1}$$

where $d=4-2\epsilon$ is the parameter of dimensional regularization. It is important to keep track of $+i0$ prescriptions because incorrect prescriptions could lead to an improper sign of the resulting integral.

For the leading-power computation, it is sufficient to consider $p^2=0$. Then the only dimensional parameter is $\omega=2(Pv)$. Also, only the good component (with respect to P) of the quark field contributes to the leading-power term. To project the corresponding component we do

$$I^T=\frac{1}{4}\mathrm{Tr}[I\gamma^-\gamma^+],\tag{B2}$$

where I is the diagram without a spinor multiplier. After projecting, the diagram decomposes into a sum of simpler scalar integrals, which have the general form

$$F(a,b,c,d,e,f,g,h) = \int \frac{d^dk}{(2\pi)^d}\frac{d^dl}{(2\pi)^d}\frac{1}{[k^2]^a[(P+k)^2]^b[l^2]^c[(P+l)^2]^d} \times \frac{1}{[(k-l)^2]^e[k\cdot v]^f[l\cdot v]^g[(k-l)\cdot v]^h}, \tag{B3}$$

where all propagators have the $+i0$ pole prescription. Next, the integrals are reduced to the set of base integrals by the integration-by-parts relations (see Refs. [39,44] for a similar example). Specifically, we have used the FIRE6 library [40]. Most parts of the base integrals are evaluated using successively one-loop integrals and are expressed with products of gamma functions. We found only two integrals with nontrivial topology. These integrals can be computed in the terms of higher-order hypergeometric functions or as an ϵ series [45] (for instance, we have used the Mellin-Barnes method). The results are

$$F(0,1,0,1,1,1,0,1) = \frac{[v^2-i0]^{-1+2\epsilon}}{[\omega-i0]^{4\epsilon}} e^{-2\gamma_E\epsilon}\left(-\frac{\zeta_2}{\epsilon}-2\zeta_2-2\zeta_3+\cdots\right), \tag{B4}$$

$$F(0,1,1,0,1,1,1,0) = \frac{[v^2-i0]^{-1+2\epsilon}}{[\omega-i0]^{4\epsilon}} e^{-2\gamma_E\epsilon}\left(-\frac{\zeta_2}{\epsilon}-6\zeta_2+3\zeta_3+\cdots\right), \tag{B5}$$

where γ_E is the Euler-Mascheroni constant and dots represent higher powers of ϵ series.

Finally, by collecting the expressions together and expanding gamma functions in ϵ we obtain the bare expressions for each diagram. For example, the diagram (B1) produces the following expansion:

$$I = a_s^2 X^{2\epsilon} e^{-2\epsilon\gamma_E} C_F\left(C_F-\frac{C_A}{2}\right)\left(\frac{1}{12\epsilon^4}+\frac{1}{3\epsilon^3} + \frac{1}{\epsilon^2}\left(\frac{5}{3}-\frac{3}{4}\zeta_2\right)+\frac{1}{\epsilon}\left(2\zeta_2-\frac{92}{9}\zeta_3+\frac{47}{6}\right) + 22\zeta_2-\frac{215}{9}\zeta_3-\frac{1031}{16}\zeta_4+\frac{211}{6}+\cdots\right), \tag{B6}$$

where $a_s = g^2/(4\pi)^{d/2}$ and $X = v^2/(\omega-i0)^2$.

[1] H.-W. Lin *et al.*, Prog. Part. Nucl. Phys. **100**, 107 (2018).
[2] M. Constantinou *et al.*, Prog. Part. Nucl. Phys. **121**, 103908 (2021).
[3] M. Constantinou *et al.*, arXiv:2202.07193.
[4] S. Rodini and A. Vladimirov, J. High Energy Phys. 09 (2023) 117.
[5] M. A. Ebert, I. W. Stewart, and Y. Zhao, J. High Energy Phys. 03 (2020) 099.
[6] X. Ji, Y. Liu, and Y.-S. Liu, Nucl. Phys. **B955**, 115054 (2020).
[7] X. Ji, Y. Liu, and Y.-S. Liu, Phys. Lett. B **811**, 135946 (2020).
[8] A. A. Vladimirov and A. Schäfer, Phys. Rev. D **101**, 074517 (2020).
[9] M. A. Ebert, S. T. Schindler, I. W. Stewart, and Y. Zhao, J. High Energy Phys. 09 (**2020**) 099.
[10] M. A. Ebert, S. T. Schindler, I. W. Stewart, and Y. Zhao, J. High Energy Phys. 04 (**2022**) 178.
[11] M. A. Ebert, I. W. Stewart, and Y. Zhao, Phys. Rev. D **99**, 034505 (2019).
[12] Q.-A. Zhang *et al.* (Lattice Parton Collaboration), Phys. Rev. Lett. **125**, 192001 (2020).
[13] M. Schlemmer, A. Vladimirov, C. Zimmermann, M. Engelhardt, and A. Schäfer, J. High Energy Phys. 08 (2021) 004.
[14] Y. Li *et al.*, Phys. Rev. Lett. **128**, 062002 (2022).
[15] M.-H. Chu *et al.* (LPC Collaboration), Phys. Rev. D **106**, 034509 (2022).
[16] H.-T. Shu, M. Schlemmer, T. Sizmann, A. Vladimirov, L. Walter, M. Engelhardt, A. Schäfer, and Y.-B. Yang, Phys. Rev. D **108**, 074519 (2023).
[17] J.-C. He, M.-H. Chu, J. Hua, X. Ji, A. Schäfer, Y. Su, W. Wang, Y. Yang, J.-H. Zhang, and Q.-A. Zhang (LPC Collaboration), arXiv:2211.02340.
[18] V. Bertone, I. Scimemi, and A. Vladimirov, J. High Energy Phys. 06 (2019) 028.
[19] I. Scimemi and A. Vladimirov, J. High Energy Phys. 06 (2020) 137.
[20] A. Bacchetta, V. Bertone, C. Bissolotti, G. Bozzi, M. Cerutti, F. Piacenza, M. Radici, and A. Signori, J. High Energy Phys. 10 (2022) 127.
[21] V. Moos, I. Scimemi, A. Vladimirov, and P. M. Zurita (to be published).
[22] I. Scimemi and A. Vladimirov, Eur. Phys. J. C **78**, 89 (2018).
[23] S. Rodini and A. Vladimirov, J. High Energy Phys. 08 (2022) 031; 12 (2022) 48.
[24] B. U. Musch, P. Hagler, J. W. Negele, and A. Schafer, Phys. Rev. D **83**, 094507 (2011).
[25] B. U. Musch, P. Hagler, M. Engelhardt, J. W. Negele, and A. Schafer, Phys. Rev. D **85**, 094510 (2012).
[26] V. S. Dotsenko and S. N. Vergeles, Nucl. Phys. **B169**, 527 (1980).
[27] P. Shanahan, M. L. Wagman, and Y. Zhao, Phys. Rev. D **101**, 074505 (2020).
[28] J.-Y. Chiu, A. Jain, D. Neill, and I. Z. Rothstein, J. High Energy Phys. 05 (2012) 084.

[29] M. G. Echevarría, A. Idilbi, and I. Scimemi, Phys. Lett. B **726**, 795 (2013).
[30] A. A. Vladimirov, Phys. Rev. Lett. **125**, 192002 (2020).
[31] S. M. Aybat and T. C. Rogers, Phys. Rev. D **83**, 114042 (2011).
[32] T. Becher and M. Neubert, Phys. Rev. D **79**, 125004 (2009); **80**, 109901(E) (2009).
[33] V. M. Braun, K. G. Chetyrkin, and B. A. Kniehl, J. High Energy Phys. 07 (2020) 161.
[34] M. G. Echevarria, I. Scimemi, and A. Vladimirov, J. High Energy Phys. 09 (2016) 004.
[35] R. Brüser, Z. L. Liu, and M. Stahlhofen, J. High Energy Phys. 03 (2020) 071.
[36] M. Neubert, Phys. Rep. **245**, 259 (1994).
[37] P. A. Baikov, K. G. Chetyrkin, A. V. Smirnov, V. A. Smirnov, and M. Steinhauser, Phys. Rev. Lett. **102**, 212002 (2009).
[38] M. G. Echevarria, I. Scimemi, and A. Vladimirov, Phys. Rev. D **93**, 054004 (2016).
[39] D. J. Broadhurst and A. G. Grozin, Phys. Rev. D **52**, 4082 (1995).
[40] A. V. Smirnov and F. S. Chuharev, Comput. Phys. Commun. **247**, 106877 (2020).
[41] Y. Su, J. Holligan, X. Ji, F. Yao, J.-H. Zhang, and R. Zhang, Nucl. Phys. **B991**, 116201 (2023).
[42] X. Ji, Y. Liu, and Y. Su, J. High Energy Phys. 08 (2023) 037.
[43] M. G. Echevarria, T. Kasemets, P. J. Mulders, and C. Pisano, J. High Energy Phys. 07 (2015) 158; 05 (2017) 73.
[44] K. G. Chetyrkin and A. G. Grozin, Nucl. Phys. **B666**, 289 (2003).
[45] V. A. Smirnov, *Analytic Tools for Feynman Integrals* (Springer, Berlin, Heidelberg, 2012), Vol. 250.